CMLS, Cell. Mol. Life Sci. 61 (2004) 1805–1815
1420-682X/04/141805-11
DOI 10.1007/s00018-004-4089-9

CMLS Cellular and Molecular Life Sciences

Research Article

Aloe-emodin prevents cytokine-induced tumor cell death: the inhibition of auto-toxic nitric oxide release as a potential mechanism

S. Mijatovic[a,*], D. Maksimovic-Ivanic[a], J. Radovic[a], D. Popadic[b], M. Momcilovic[a], L. Harhaji[a], D. Miljkovic[a] and V. Trajkovic[b]

[a] Department of Neurobiology and Immunology, Institute for Biological Research, 29. Novembra 142, 11000 Belgrade (Serbia and Montenegro), Fax: +381 11 265 7258, e-mail: mamas@yubc.net
[b] Institute of Microbiology and Immunology, School of Medicine, University of Belgrade, Belgrade (Serbia and Montenegro)

Received 2 March 2004; received after revision 29 April 2004; accepted 26 May 2004

Abstract. Aloe-emodin (AE) is a plant-derived hydroxyanthraquinone with potential anticancer activity. We investigated the ability of AE to modulate survival of mouse L929 fibrosarcoma and rat C6 astrocytoma cells through interference with the activation of inducible nitric oxide (NO) synthase (NOS) and subsequent production of tumoricidal free radical NO. Somewhat surprisingly, AE in a dose-dependent manner rescued interferon-γ + interleukin-1-stimulated L929 cells from NO-dependent killing by reducing their autotoxic NO release. The observed protective effect was less pronounced in C6 cells, due to their higher sensitivity to a direct toxic action of the drug. AE-mediated inhibition of tumor cell NO release coincided with a reduction in cytokine-induced accumulation of transcription and translation products of genes encoding inducible NOS and its transcription factor IRF-1, while activation of NF-κB remained unaltered. These data indicate that the influence of AE on tumor growth might be more complex that previously recognized, the net effect being determined by the balance between the two opposing actions of the drug: its capacity to directly kill tumor cells, but also to protect them from NO-mediated toxicity.

Key words. Aloe-emodin; nitric oxide; iNOS; tumor.

The production of the highly reactive free radical nitric oxide (NO) by inducible NO synthase (iNOS)-mediated oxidation of intracellular L-arginine has been recently recognized as a major antitumor mechanism of innate immunity [1, 2]. The NO released by cytokine-activated macrophages and natural killer (NK) cells presents a powerful antiproliferative and proapoptotic signal for both human and animal tumor cells in vitro [3, 4], and the functional iNOS gene is required for in vivo inhibition of tumor growth and metastasis [5, 6]. The mechanism of NO-mediated tumor cell apoptosis involves accumulation of the tumor suppressor protein p53, damage of mitochondrial functions, alterations in the expression of antiapoptotic molecules belonging to the Bcl-2 family, activation of the caspase cascade, and DNA fragmentation [4]. In addition to cells of innate immunity, many tumor cells possess the ability to engage the iNOS enzymatic system and produce large amounts of NO. Moreover, recent in vivo studies directly implicate tumor cell-derived NO as an important autocrine/paracrine factor in the limitation of tumor progress [7–9].

* Corresponding author.

In light of the above data, modulation of host NO release could profoundly influence the efficiency of an antitumor therapy. Indeed, such an assumption is at the core of various experimental immunostimulatory therapies that employ iNOS-inducing cytokines like interleukin (IL)-2 or IL-12 [10-13]. Interestingly, several primarily non-immune-based therapeutic strategies, including ionizing irradiation and administration of chemotherapeutics such as taxol or cisplatin, also appears to owe their antitumor effect at least in part to their ability to induce iNOS and subsequent NO synthesis in the host cells [14–16]. On the other hand, antraquinones, potentially useful antitumor agents from Chinese herbs, have been recently demonstrated to markedly suppress the induction of iNOS and subsequent NO release in macrophage cultures [17–19]. One of the most potent of these antraquinones was emodin (3-methyl-1,6,8-trihydroxyanthraquninone; fig. 1) which also displayed powerful anti-inflammatory and immunosuppressive effects in various experimental settings [20–24]. Although the anti-inflammatory properties of emodin, and particularly the suppression of iNOS-mediated NO release, might influence its efficiency in restricting tumor growth, such a hypothesis has not been directly tested thus far.

In the present study, we investigated the ability of aloe-emodin (AE; 1,8-dihydroxy-3-hydroxymethyl-anthraquinone; fig. 1), a tumoricidal hidroxyantraquinone structurally very similar to emodin, to affect iNOS-dependent NO release by tumor cells. Our data indicate that in certain conditions, AE could significantly improve tumor cell survival by reducing the production of NO.

Materials and methods

Reagents

Fetal calf serum (FCS), RPMI-1640, and phosphate-buffered saline (PBS) were from Flow Laboratories (Irvine, UK). Rat and mouse recombinant interferon (IFN)-γ were obtained from Sigma (St. Louis, Mo.), while human IL-1β was from R&D Systems (Minneapolis, Minn.). Cycloheximide was obtained from U.S. Biochemical Corporation (Cleveland, Ohio). Moloney leukemia virus reverse transcriptase and Taq polymerase were purchased from Eurogentec (Seraing, Belgium), while RNA Isolator was provided by Genosys (Woodlands, Tex.). Random primers were from Pharmacia (Uppsala, Sweden). Rabbit anti-mouse IRF-1 and anti-rat phospho-IκB were purchased from Santa Cruz Biotechnology (Santa Cruz, Calif.), while HRP-conjugated anti-rabbit IgG was from USB (Cleveland, Ohio). Rabbit anti-mouse iNOS, dimethyl sulfoxide (DMSO), 3-(4,5-dimethylthiazol-2-yl)-2,5-diphenyltetrazolium bromide (MTT), 3-morpholinosydnonimine (SIN-1) and AE were obtained from Sigma. AE was stored at –20 °C at a concentration of 200 mM in DMSO, and was diluted in culture medium immediately before use.

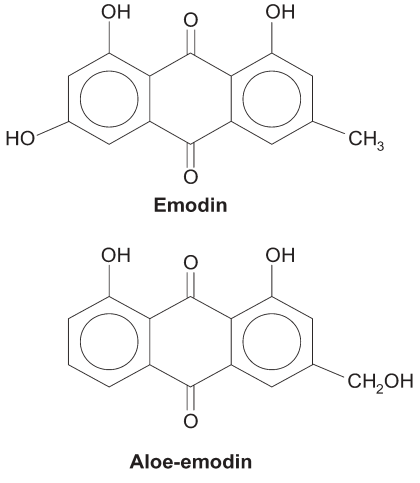

Figure 1. Chemical structure of emodin and aloe-emodin.

Cells and cultures

The murine fibrosarcoma cell line L929 and rat astrocytoma cell line C6 were obtained from the European Collection of Animal Cell Cultures (Salisbury, UK), and grown in HEPES-buffered RPMI-1640 medium supplemented with 5% FCS, 2 mM L-glutamine, antibiotics, 0.1% sodium pyruvate (culture medium) at 37 °C in a humidified atmosphere with 5% CO_2. Plastic-adherent fibroblast-like short-term cell lines were derived from spleens of CBA mice (animal facility of the Institute for Biological Research, Belgrade, Serbia and Montenegro), as previously described [25]. Primary astrocytes were isolated from mixed glial cell cultures prepared from brains of newborn AO rats (animal facility of the Institute for Biological Research, Belgrade, Yugoslavia), as previously described [26]. Astrocytes were maintained in culture medium supplemented with 6 g/l glucose. After a conventional trypsinization procedure, C6 cells, L929 cells, astrocytes or fibroblasts were incubated in flat-bottom 96- or 24-well plates (Flow Laboratories) for NO production and mRNA isolation, respectively, at conditions indicated in the figure legends. Control cell cultures contained the amount of DMSO (0.01%, 0.02%, or 0.04%) corresponding to its content in the solution with the highest concentration of AE used in the particular experiment (20, 40, or 80 μM, respectively). Results obtained with DMSO-containing controls did not differ from those of untreated control cells (data not shown).

Flow cytometry analysis of AE uptake

AE is a fluorescent compound with maximum excitation at 410 nm and a maximum emission wavelength at 510 nm [27]. The cellular uptake of the drug was examined by flow cytometry as previously described [27]. Briefly, control and AE-treated cells were detached by scraping, and

washed three times in PBS before analysis on a FACS Calibur flow cytometer (BD, Heidelberg, Germany).

Determination of cell viability by MTT and crystal violet assay

Cellular respiration, as an indicator of cell viability, was assessed by the mitochondrial-dependent reduction of MTT to formazan [28]. At the end of the culture period, MTT solution was added to cell cultures at a final concentration of 0.5 mg/ml and cells were incubated for an additional 1 h. Thereafter, medium was removed and cells were lysed in DMSO. The conversion of MTT to formazan by metabolically viable cells was monitored by an automated microplate reader at 570 nm. Alternatively, cell viability was assessed by the crystal violet assay that measures the number of viable adherent cells [29]. At the end of incubation, cells were washed with PBS to remove non-adherent cells, fixed with methanol and stained with 1% crystal violet solution at room temperature for 10 min. Plates were thoroughly washed with PBS, 33% acetic acid was added to each well, and absorbance of dissolved dye, corresponding to the number of viable cells, was measured in a microplate reader at 570 nm.

Nitrite measurement

Nitrite accumulation, an indicator of NO production, was measured in cell culture supernatants using the Griess reagent [30]. Briefly, samples of culture supernatants were mixed with an equal volume of Griess reagent (a mixture at 1:1 of 0.1% naphthylenediamine dihydrochloride and 1% sulfanilamide in 5% H_3PO_4) and incubated at room temperature for 10 min. The absorbance at 570 nm was measured in a microplate reader. The nitrite concentration was calculated from a $NaNO_2$ standard curve.

Determination of iNOS and IRF-1 mRNA by RT-PCR

Total RNA from cell cultures was isolated with RNA Isolator, according to the manufacturer's instructions. RNA was reverse transcribed using Moloney leukemia virus reverse transcriptase and random primers. PCR amplification of cDNA with primers specific for iNOS/IRF-1 and GAPDH as a housekeeping gene, was carried out in the same tube in a Thermojet (Eurogentec) thermal cycler as follows: 30 s of denaturation at 95 °C, 30 s of annealing at 53 °C, and 30 s of extension at 72 °C. The number of cycles (30 for both iNOS and iRF-1, and 25 for GAPDH) ensuring non-saturating PCR conditions was established in preliminary experiments. For iNOS, the sense primer was 5′-AGAGAGATCCGGTTCACA-3′, and the antisense primer was 5′-CACAGAACTGAGGGTACA-3′, corresponding to positions 88–105 and 446–463, respectively, of the published rat iNOS mRNA sequence (GenBank accession number S71597); the PCR product was 376 bp long. For IRF-1, the primers were: sense, 5′-GACCAGAGCAGGAACAAG-3′; antisense, 5′-TAACTTCCCTTCCTCATCC-3′, corresponding to positions 483–500 and 881–899, respectively, of the published rat IRF-1 mRNA sequence (M34253); the PCR product was 417 bp long. The primers for GAPDH were: sense, 5′-GAAGGGTGGGGCCAAAAG-3′; antisense, 5′-GGATGCAGGGATGATGTTCT-3′, corresponding to positions 371–388 and 646–665 of the published rat GAPDH mRNA sequence (AB017801); the PCR product was 295 bp long. PCR products were visualized by electrophoresis on an agarose gel stained with ethidium bromide.

Western blot analysis of iNOS expression

Cells were collected from tissue culture flasks by scraping, washed with cold PBS, and lysed in ice-cold buffer containing 0.1 M NaCl, 0.01 M Tris-Cl (pH 7.6), 0.001 M EDTA (pH 8.0), 100 µg/ml PMSF, and 1 µg/ml aprotinin. After centrifugation at 3200 g for 5 min (4 °C), concentration of proteins in cell lysate supernatants was measured by the Bradford assay. The samples were mixed with 6 × gel-loading buffer (0.3 M Tris-Cl pH 6.8, 10% SDS, 30% glycerol, 0.84 mM 2-mercaptoethanol, and 0.2% bromophenol blue), and the mixture was boiled for 5 min. SDS-PAGE electrophoresis of samples containing 50 µg of proteins was conducted through a 5% stacking and 8% resolving gel in electrophoresis buffer (25 mM Tris, 192 mM glycine, and 0.1% SDS), along with a prestained protein marker (New England BioLabs). The resolved proteins were then transferred onto Hybond ECL nitrocellulose membrane (Amersham Life Sciences, Amersham, UK) at 1 mA/cm^2 of membrane, using transfer buffer (25 mM Tris, 192 mM glycine, 0.1% SDS, and 20% methanol). After overnight blocking at 4 °C with 5% non-fat milk in PBS containing 0.1% Tween 20, blots were incubated for 1 h at room temperature with anti-iNOS antibody (1:10,000 in blocking buffer). The membranes were then thoroughly washed with PBS/Tween 20, and incubated for 1 h at room temperature with HRP-conjugated anti-rabbit IgG (1:2500 in blocking buffer). After washing, peroxidase activity corresponding to a 130-kDa iNOS band was detected by 3,3′,5,5′-tetramethyl-benzidine (TMB) liquid substrate for membranes (Sigma).

Cell-based ELISA for iNOS, IRF-1, and phospho-IκB

The expression of iNOS, IRF-1, and phospho-IκB was determined by a slightly modified original protocol for the cell-based ELISA [31]. After cultivation, cells were fixed with 4% paraformaldehyde in PBS for 20 min at room temperature and washed three times with PBS containing 0.1% Triton X-100 (PBS/T). Endogenous peroxidase was quenched with 0.6% H_2O_2 in PBS/T for 20 min, and cells were washed three times in PBS/T. Following blocking with 10% FCS in PBS/T for 1 h, cells were incubated for 1 h at 37 °C with the primary antibody in PBS/T containing 1% BSA. After washing the cells four times with PBS/T for 5 min, they were incubated for 1 h

at 37 °C with secondary antibody (anti-rabbit-HRP; 1:2500) in PBS/T containing 1% BSA. Subsequently, cells were washed and incubated with 200 µl of a solution containing 0.4 mg/ml OPD, 11.8 mg/ml $Na_2HPO_4 \times 2H_2O$, 7.3 mg/ml citric acid, and 0.015% H_2O_2 for 30 min at room temperature in the dark. The reaction was stopped with 50 µl of 3 M HCl, and the absorbance at 492 nm was determined in a microplate reader. The data were corrected for differences in cell number by staining the wells with crystal violet after the ELISA procedure, as described in the original protocol [31].

Statistical analysis

To analyze the significance of the differences between various treatments performed in triplicate, we used analysis of variance (ANOVA), followed by the Student-Newman-Keuls test. A p value less than 0.05 was considered significant.

Results

AE inhibits growth of non-confluent C6 and L929 cells

Taking advantage of the fact that AE emits relatively intense green fluorescence, we first examined by flow cytometry the ability of L929 fibrosarcoma and C6 astrocytoma cells to internalize the drug. Incubation of both C6 and L929 cells with AE gave rise to an intense fluorescence emission, suggesting a significant cellular uptake of the drug (fig. 2A). We next investigated whether AE internalization might influence the growth of tumor cells. As shown in figure 2C, non-confluent tumor cells initially proliferated vigorously and attained almost total confluence after 48 h of incubation. However, the growth of both L929 and C6 cells was markedly retarded by AE in a dose-dependent manner (fig. 2C). The data obtained by microscopic observation were confirmed by the results of MTT and crystal violet assays (fig. 2B), which measure cell respiration or number of viable adherent cells, respectively.

AE improves the survival of confluent tumor cells by downregulating NO release

As non-confluent tumor cells produced very low amounts of NO (data not shown), the influence of AE on tumor cell NO release was investigated in confluent cell cultures. While resting cells did not produce detectable amounts of NO (nitrite accumulation < 2 µM), stimulation with well-known iNOS-inducing cytokines, IFN-γ and IL-1, caused significant NO release in L929 and C6 cell cultures (16.1 ± 1.3 µM and 8.9 ± 0.9 µM, respectively). The addition of AE reduced cytokine-triggered NO synthesis in both cell types in a dose-dependent fashion (fig. 3A, B), but the effect was more pronounced in L929 cells. While the effects of IFN-γ and IL-1 on tumor cell NO production were dose dependent, the inhibitory action of AE could not be surmounted merely by increasing the cytokine concentration (data not shown). Interestingly, confluent tumor cell cultures were far less sensitive to AE toxicity than non-confluent ones, with C6 cells becoming partly, and L929 cells completely resistant to the toxic action of the drug (fig. 3C, D). Cytokine stimulation significantly decreased tumor cell respiration (fig. 3C, D), and we have previously reported that this effect was mainly dependent on concomitant induction of NO [32, 33]. Accordingly, downregulation of NO release by AE completely neutralized the toxic effect of cytokine stimulation in AE-resistant cultures of confluent L929 cells (fig. 3C). Although this protective effect of AE was not obvious in C6 cells, the viability of cytokine-treated C6 cells, in contrast to unstimulated ones, did not further deteriorate upon addition of AE (fig. 3D). This indicates that the toxic effect of the drug on C6 cells might have been counteracted by its ability to suppress detrimental NO release. The protective action of AE on L929 cells was further confirmed by microscopic observation of tumor cell cultures. In accordance with data obtained with the MTT assay, the combination of IFN-γ and IL-1 markedly reduced the number of L929 cells, while this effect of cytokine stimulation was completely surmounted in the presence of AE (fig. 3E). A similar pattern was observed if aminoguanidine, an inhibitor of iNOS-mediated NO production [34], was used instead of AE (fig. 3E), which is consistent with the assumption that the protective effect of AE on L929 cells was due to a block of NO release. The addition of *Escherichia coli* Lipopolysaccharide (LPS) (1 µg/ml) or the LPS-inactivating agent polymyxin B (5 µg/ml) failed to mimic or block, respectively, the observed effects of AE (data not shown), thus excluding LPS contamination as responsible for the drug action. To exclude the possibility that AE might directly interfere with the toxic action of NO, we tested its influence on tumor cell killing induced by exogenous NO generated by the NO-releasing chemical SIN-1. As expected, SIN-1 reduced the viability of both L929 and C6 cells in a dose-dependent manner (fig. 4A). However, AE was unable to improve survival of either tumor cell line in this setting (fig. 4B, C), which confirmed the inability of the drug to antagonize the toxicity of already generated NO.

AE suppresses the induction of iNOS and IRF-1 in tumor cells

We next examined the mechanisms responsible for AE-mediated suppression of NO release by tumor cells. To assess possible influence of AE on iNOS catalytic activity, the drug was added to C6 and L929 cells in which iNOS had already been induced by 24-h pretreatment with IFN-γ and IL-1β, while any further iNOS expression

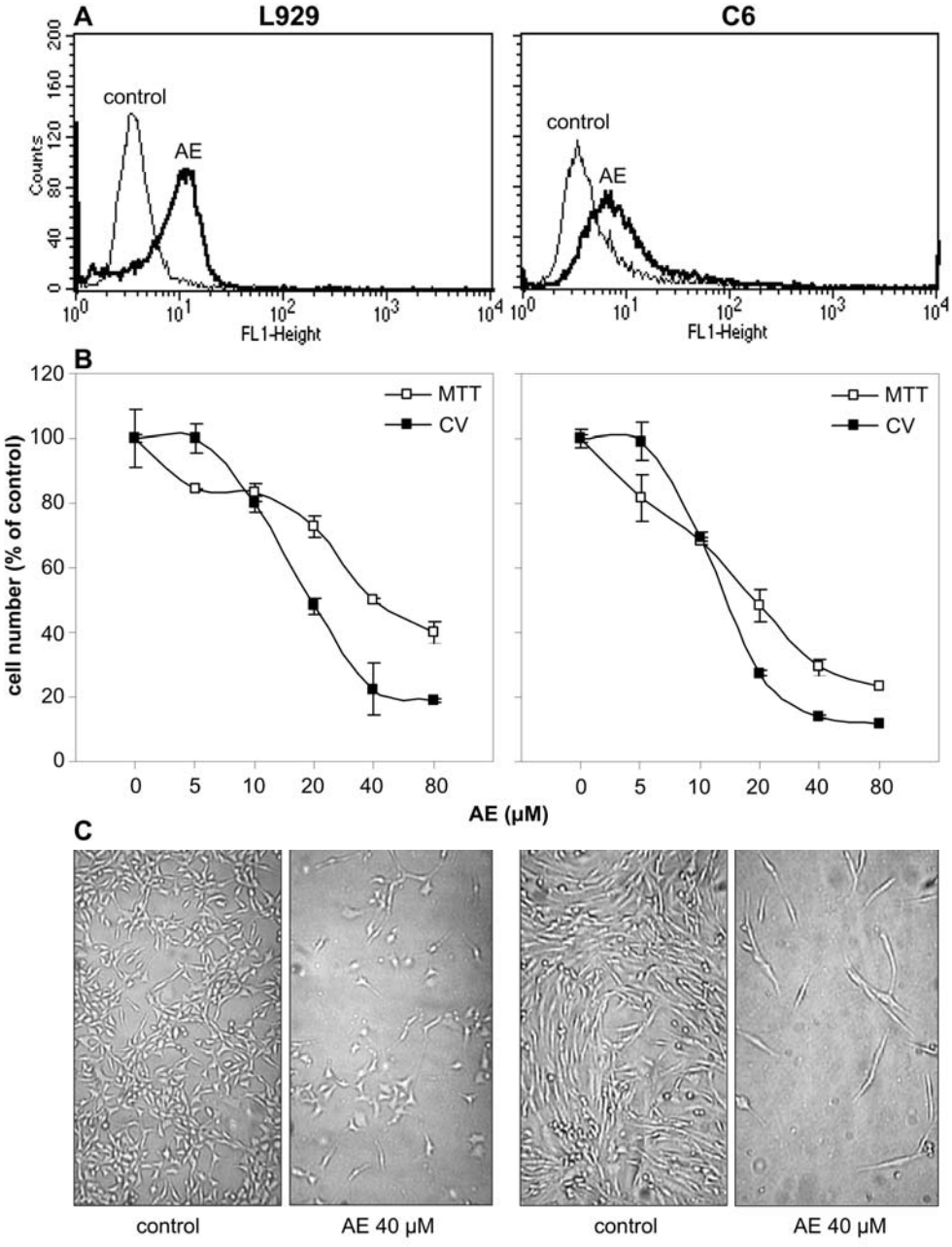

Figure 2. Cytotoxic effect of AE on non-confluent C6 and L929 cells. (*A–C*) L929 or C6 cells (1×10^4/well) were incubated with AE for 48 h. (*A*) Drug uptake was evaluated by analyzing the ability of the cells treated with 20 μM AE and untreated cells (control) to emit green fluorescence. (*B*) Tumor cell number in the cultures treated with different doses of AE was assessed by MTT or crystal violet (CV) assay. The results, representative of five independent experiments, presented as % of the control value, are means ± SD of triplicate observations (* $p < 0.05$). (*C*) The reduction of tumor cell number by AE (40 μM) was assessed by light microscopy.

was blocked with the translation inhibitor cycloheximide. Under these conditions, AE failed to decrease NO production (fig. 5A), which suggested that the drug might affect the expression of the iNOS gene rather than its enzymatic activity. Therefore, we investigated the effect of AE on expression of mRNA for iNOS and its important transcription factor IRF-1 in C6 cells. Under the PCR conditions employed, the levels of iNOS and IRF-1 mRNA were not detectable in untreated cells, but they were markedly elevated upon stimulation with IFN-γ and IL-1 (fig. 5B). The presence of AE during cytokine stimulation significantly inhibited the accumulation of both iNOS and IRF-1 transcripts (fig. 5B). This finding was paralleled by the inhibitory effect of AE on (IFN-γ + IL-1-induced expression of iNOS and IRF-1 protein products in L929 cells, as determined by cell-based ELISA for

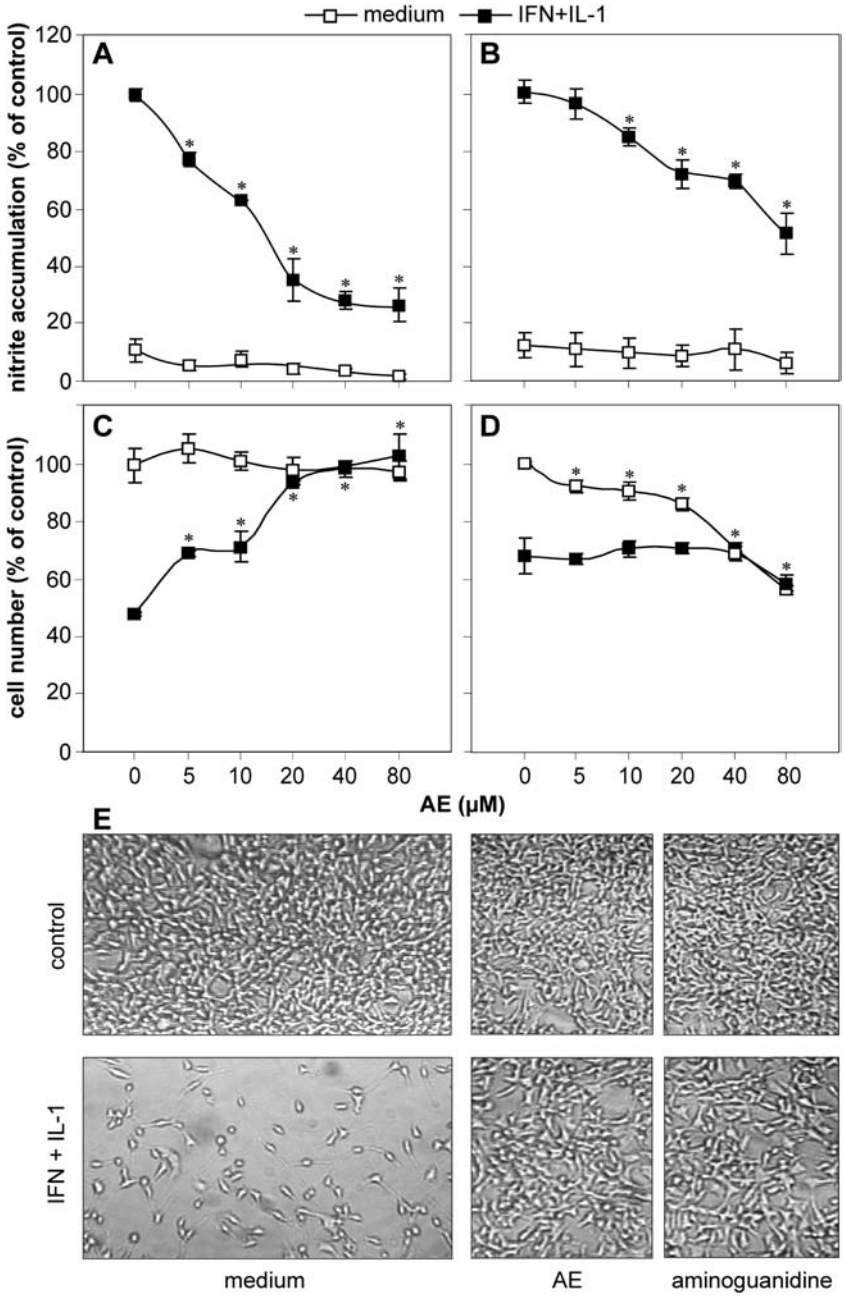

Figure 3. The effect of AE on NO production and viability of confluent tumor cells. Confluent L929 (*A*, *C*) or C6 cells (*B*, *D*) were stimulated with IFN-γ (250 U/ml) and IL-1 (10 ng/ml), in the presence or absence of AE. Nitrite concentration in cell culture supernatants (*A*, *B*) and cell number (MTT reduction) (*C*, *D*) were determined after 48 h. Results, representative of four separate experiments, presented as % of the control value, are given as the mean ± SD of triplicate observations (* $p < 0.05$). (*E*) The photographs show that 48 h treatment with either AE (20 μM) or the iNOS inhibitor aminoguanidine (1 mM) prevents (IFN-γ + IL-1)-mediated reduction of cell number in confluent L929 cultures.

both proteins (fig. 5C) and Western blot for iNOS (fig. 5D). Similar results were obtained when iNOS/IRF-1 mRNA or protein levels were examined in L929 or C6 cells, respectively (data not shown). These results indicate that AE might suppress tumor cell NO release at least partly by interfering with IRF-1-dependent expression of the iNOS gene.

AE does not affect cytokine-induced activation of NF-κB in tumor cells

IFN-γ-activated IRF-1 mediates iNOS transcription in synergy with NF-κB, another transcription factor induced mainly by proinflammatory cytokines such as IL-1 [35]. Thus, we next investigated the ability of AE to interfere with (IFN-γ + IL-1)-triggered activation of NF-κB in C6

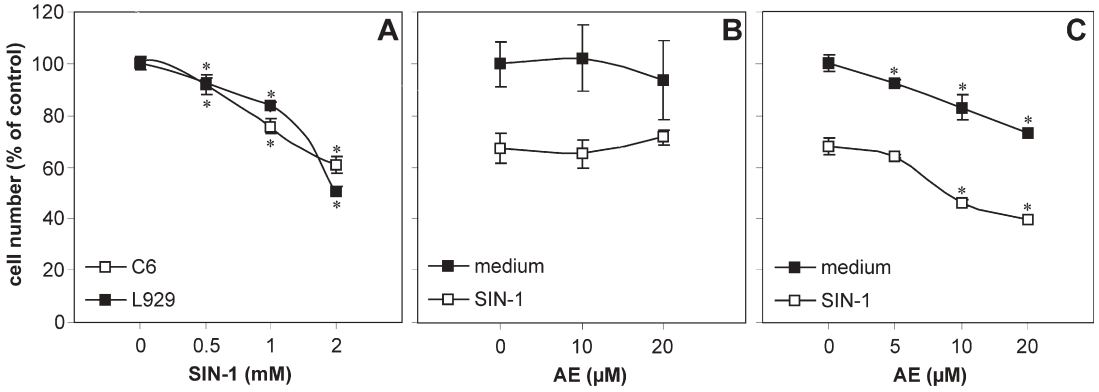

Figure 4. AE does not affect the toxicity of exogenous NO in confluent L929 and C6 cells. Confluent L929 (*A*, *B*) or C6 cells (*A*, *C*) were incubated for 24 h with different doses (*A*) or 2 mM of SIN-1 (*B*, *C*), in the absence or presence of AE (*B*, *C*). Cell number was determined by MTT assay. Results, representative of three independent experiments, presented as % of the control value, are means ± SD of triplicate observations (* $p < 0.05$).

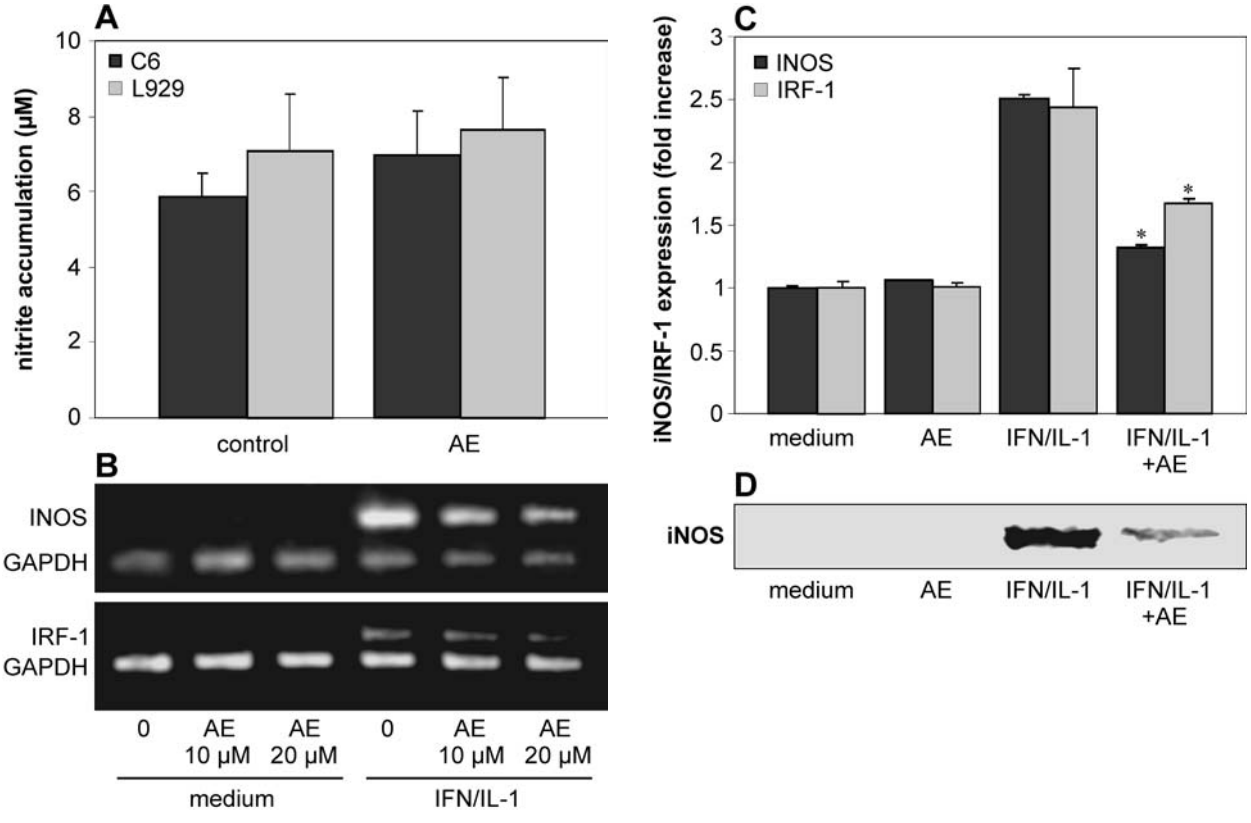

Figure 5. AE inhibits iNOS and IRF-1 expression in tumor cells. (*A*) To induce iNOS, confluent C6 and L929 cells were stimulated for 24 h with 250 U/ml IFN-γ + 10 ng/ml IL-1β. Afterwards, cells were thoroughly washed and cultured for an additional 24 h in fresh medium containing 5 μg/ml cycloheximide, in the absence (control) or presence of AE (20 μM). Nitrite accumulation is presented as the mean ± SD of triplicate observations from a representative of three separate experiments. (*B*) C6 cells (3×10^5/well) were stimulated with IFN-γ + IL-1, in the presence or absence of AE. After 6 h, total RNA was isolated and RT-PCR amplification of iNOS and IRF-1 cDNA was performed. Similar results were obtained in another two experiments. (*C*) The amounts of iNOS and IRF-1 proteins were determined by cell-based ELISA in confluent L929 cells stimulated for 24 h with IFN-γ + IL-1, in the presence or absence of AE. Results from a representative of three separate experiments are presented as fold increase in comparison to untreated cells, and are given as the mean ± SD of triplicate observations (* $p < 0.05$). (*D*) Western blot analysis of iNOS expression in L929 cells (5×10^6/sample) stimulated for 24 h with IFN-γ + IL-1 in the presence or absence of AE (20 μM). A single band corresponding to 130-kDa iNOS protein was observed.

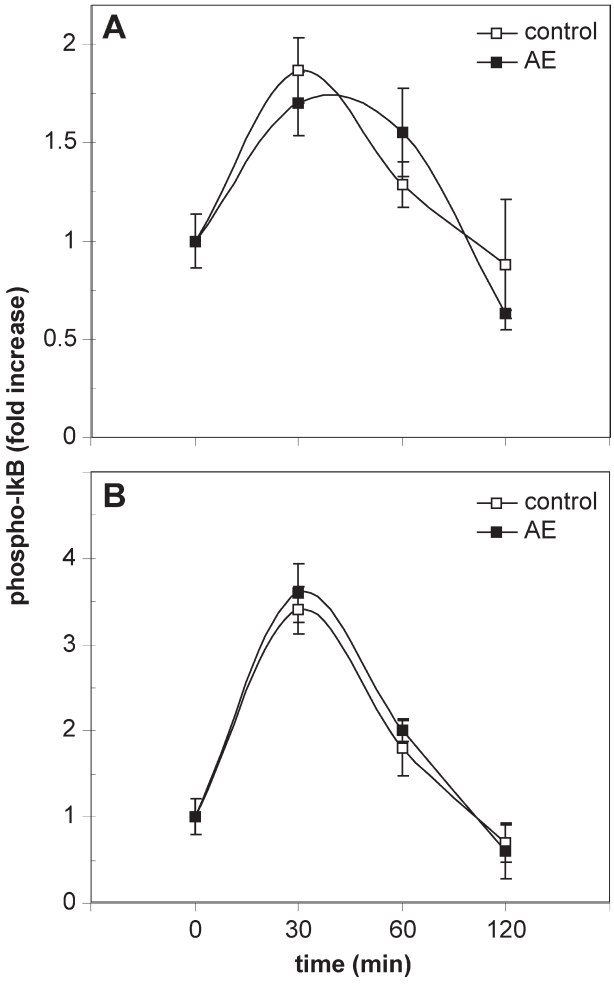

Figure 6. AE does not block cytokine-induced NF-κB activation in tumor cells. Confluent L929 (*A*) or C6 cells (*B*) were incubated with 250 U/ml IFN-γ + 10 ng/ml IL-1β, in the presence or absence of AE (20 μM). The intracellular concentration of phospho-IκB was assessed at different time points by cell-based ELISA. Results from a representative of three separate experiments are presented as fold increase (mean ± SD of triplicate observations) relative to values obtained in untreated cultures (0 min).

and L929 cells. Since activation and subsequent nuclear translocation of constitutively expressed NF-κB is mediated by phosphorylation of its inhibitor IκB [35], we employed a cell-based ELISA to measure the amount of phosphorylated IκB as an indicator of NF-κB activation. As expected, stimulation of both C6 and L929 cells with cytokines led to a rapid increase in the intracytoplasmic concentration of phospho-IκB (fig. 6), presumably reflecting the activation of NF-κB. However, while the amount of phospho-IκB returned to basal levels 2 h after stimulation, AE did not significantly affect the phospho-IκB concentration at any of the time points tested (fig. 6). Thus, AE-mediated interference with iNOS expression in C6 and L929 cells probably does not involve inhibition of NF-κB activation.

AE inhibits NO production in primary astrocytes and fibroblasts

Finally, we sought to determine whether the inhibitory effect of AE on NO synthesis was specific for tumor cells, or could operate in the corresponding primary cells as well. We therefore assessed the influence of AE on (IFN-γ + IL-1)-induced NO production in rat primary astrocytes and mouse primary fibroblasts. While both cell types produced large amounts of NO upon cytokine stimulation, the presence of AE dose-dependently suppressed the observed NO release (fig. 7A, B). However, the viability of astrocytes and fibroblasts remained largely unaffected regardless of cytokine stimulation or the presence of AE (fig. 7C, D), indicating that primary cells might be much less sensitive to the NO and AE toxicity than their transformed counterparts.

Discussion

The hydroxyantraquinones emodin and AE are the most potent herbal antitumor agents with a strong capacity to induce programmed cell death and/or suppress proliferation in several types of tumor cell lines [27, 36–40]. Both chemicals were able to trigger apoptosis by blocking the antiapoptotic and promoting the proapoptotic action of Bcl-2 family members and, consequently, caspases 3, 8, and 9 [38–40]. In the present paper, we extend these findings on AE antitumor action to fibrosarcoma L929 cells and the astrocytoma cell line C6, while their non-transformed counterparts were resistant to the toxic action of the drug. Interestingly, confluent tumor cells were markedly less sensitive to the toxic effect of AE, indicating that cell-to-cell contact might somehow interfere with the importantly antitumor action of AE. We demonstrate for the first time the somewhat surprising ability of AE to improve the survival of confluent tumor cells by down-regulating their release of tumoricidal free radical NO.

Although the NO-producing enzyme iNOS in certain conditions could be controlled through interference with its translation or catalytic activity, it is mainly regulated at the transcriptional level [2]. Accordingly, the inhibitory action of AE on tumor cell NO production in our experiments was a consequence of a reduced expression of the iNOS gene, rather than interference with iNOS enzymatic activity. Optimal transcription of iNOS gene depends on a coordinate binding of the transcription factors IRF-1 and NF-κB to their consensus sequences in the iNOS promoter [41]. Emodin has been reported to inhibit TNF-induced activation of NF-κB in human vascular endothelial cells [42]. However, although emodin also inhibited LPS-triggered iNOS expression in mouse macrophages [17–19], this effect apparently did not involve interference with NF-κB activation [17]. The data provided in the present report indicate that AE-mediated

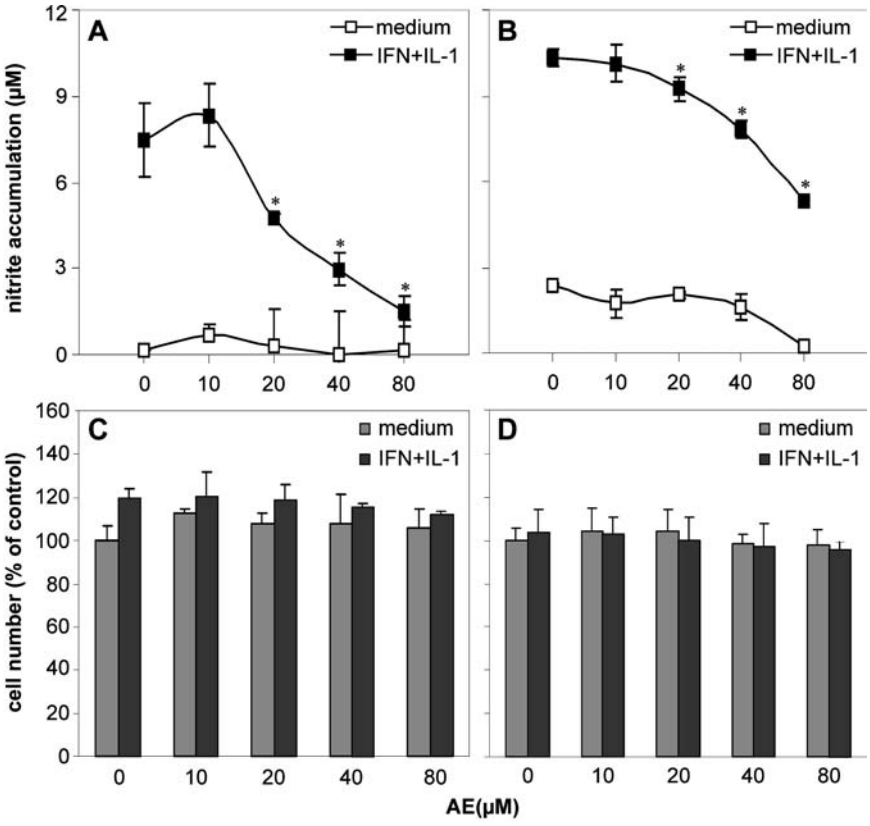

Figure 7. AE inhibits NO production in primary astrocytes and fibroblasts. Rat primary astrocytes (*A*, *C*) and mouse primary fibroblasts (*B*, *D*) (both 7×10^5/well) were stimulated with IFN-γ (250 U/ml) and IL-1 (10 ng/ml), in the presence or absence of different concentrations of AE. Nitrite accumulation (*A*, *B*) and cell number (MTT reduction) (*C*, *D*) were determined after 48 h of incubation, and results from a representative of three independent experiments are presented as means ± SD of triplicate observations (*$p < 0.05$).

suppression of (IFN-γ + IL-1)-induced iNOS induction in L929 and C6 cells might at least in part depend on a concomitant block in the activation of IRF-1, but not NF-κB. Whereas our data could not exclude the possibility that AE might interfere with NF-κB transactivating properties by acting downstream of NF-κB activation, the AE-mediated block of IRF-1 induction is consistent with the recently described ability of emodin to interfere with the protein tyrosine kinase activity [36, 37, 43]. Janus kinase (JAK)-mediated tyrosine phosphorylation is required for IFN-γ-triggered activation of transcription factors belonging to the signal transducer and activator of transcription (STAT) family, which control IRF-1 transcription and subsequent iNOS induction in astrocytes, fibroblasts, and macrophages [44–46]. This could also partly explain the emodin-mediated block of macrophage iNOS activation by LPS, since LPS has been reported to activate IRF-1 in macrophages [47]. However we cannot exclude that AE and emodin might employ distinct mechanisms for the suppression of iNOS induction. The exact mechanisms underlying the inhibitory action of AE on iNOS expression in tumor cells and macrophages are currently under investigation in our laboratory.

As in many other tumor cell types, cytokine-induced death of L929 and C6 cells in vitro depends mainly on the autocrine/paracrine toxic action of NO [32, 33]. However, while downregulation of NO release by AE completely rescued cytokine-treated L929 cells, a similar protective effect was apparently absent in C6 cultures. This could be due to the somewhat lower potential of AE for the suppression of NO release in the latter cells, as well as to the fact that confluent C6 cells, unlike L929 cells, were still sensitive to the toxic action of AE alone. Nevertheless, although AE has clearly shown an additive cytotoxic effect with exogenous NO released by NO donors, such a pattern was not observed in cytokine-treated C6 cells whose viability did not further decline upon addition of AE. Thus, the absence of collaboration between endogenous NO and AE in the killing of C6 cells might have actually been a consequence of the protective AE-mediated inhibition of NO release. This is consistent with a logical assumption that the efficiency of AE in rescuing tumor cells from endogenous NO would be limited by the sensitivity of tumor cells to the toxic action of AE alone. The net effect of AE on tumor cell survival in vitro would therefore be determined by the two opposing actions of the drug:

the induction of tumor cell death and tumor protection via interference with NO release. While aware of the limitations of our somewhat reductionist approach, we propose that the latter effect might prevail in situations in vivo where solid tumors (presumably resembling confluent cultures in vitro) are heavily infiltrated with immune cells (macrophages, T and NK cells) that would provide the cytokines (IFN-γ, IL-1, tumor necrosis factor) required for iNOS induction and tumoricidal NO release. However, the actual consequences of such AE-mediated inhibition of tumor cell NO synthesis could be much more complex, due to the recently recognized multifaceted role of NO in tumor progression. Whereas NO restricts the growth of NO-sensitive tumors, tumor cell-derived NO has been shown to facilitate development and metastasis of NO-resistant tumors through mechanisms that mainly involve angiogenesis, vasodilatation, or protection from other apoptotic stimuli [4, 6, 48, 49]. While this implies that AE might be more efficient in the treatment of NO-resistant tumors, of interest would be to examine whether down-regulation of NO release might actually contribute to the anti-tumor properties of AE in certain conditions.

The work by both us and others indicates that signaling pathways that control iNOS induction in tumor cells, including C6 and L929 cells, might differ from those operative in their non-transformed counterparts [50, 51]. However, the effect of AE in the present study was not confined to tumor cells, because it efficiently inhibited NO production in cytokine-stimulated primary astrocytes and fibroblasts. This indicates that modulation of NO release by surrounding resident cells might contribute to the effect of AE on tumor growth. Furthermore, these data suggest that inhibition of iNOS induction in resident cells might protect them from deleterious NO release, thus partly explaining the beneficial effects of the drug in various models of inflammatory disorders. As NO evidently plays an important and complex role in both inflammation and tumor progress, the possible contribution of an AE-mediated block of iNOS activation to the therapeutic properties of the drug seems worthy of further investigation, with examination of its effects on NO production in human cells as a first step in that direction.

Acknowledgements. This work was supported by the Ministry of Science, Technology and Development of the Republic of Serbia (Grants 1664 and 2020).

1 Cifone M. G., Cironi L., Meccia M. A., Roncaioli P., Festuccia C., De Nuntiis G. et al. (1995) Role of nitric oxide in cell-mediated tumor cytotoxicity. Adv. Neroimunol. **5:** 443–461
2 MacMicking J., Xie Q. W. and Nathan C. (1997) Nitric oxide and macrophage function. Annu. Rev. Immunol. **15:** 323–350
3 Brune B., Knethen A. von and Sandau K. B. (1999) Nitric oxide (NO): an effector of apoptosis. Cell. Death. Differ. **6:** 969–975
4 Umansky V. and Schirrmacher V. (2001) Nitric oxide-induced apoptosis in tumor cells. Adv. Cancer Res. **82:** 107–131
5 Wei D., Richardson E. L., Zhu K., Wang L., Le X., He Y. et al. (2003) Direct demonstration of negative regulation of tumor growth and metastasis by host-inducible nitric oxide synthase. Cancer Res. **63:** 3855–3859
6 Shi Q., Xiong Q., Wang B., Le X., Khan N. A. and Xie K. (2000) Influence of nitric oxide synthase II gene disruption on tumor growth and metastasis. Cancer Res. **60:** 2579–2583
7 Xie K., Huang S., Dong Z., Juang S. H., Gutman M., Xie Q. W. et al. (1995) Transfection with the inducible nitric oxide synthase gene suppresses tumorigenicity and abrogates metastasis by K-1735 murine melanoma cells. J. Exp. Med. **181:** 1333–1343
8 Juang S. H., Xie K., Xu L., Shi Q., Wang Y., Yoneda J. et al. (1998) Suppression of tumorigenicity and metastasis of human renal carcinoma cells by infection with retroviral vectors harboring the murine inducible nitric oxide synthase gene. Hum. Gene Ther. **9:** 845–854
9 Hu D. E., Dyke S. O., Moore A. M., Thomsen L. L. and Brindle K. M. (2004) Tumor cell-derived nitric oxide is involved in the immune-rejection of an immunogenic murine lymphoma. Cancer Res. **64:** 152–161
10 Jyothi M. D. and Khar A. (2000) Interleukin-2-induced nitric oxide synthase and nuclear factor-κB activity in activated natural killer cells and the production of interferon-γ. Scand. J. Immunol. **52:** 148–155
11 Sadanaga N., Nagoshi M., Lederer J. A., Joo H. G., Eberlein T. J. and Goedegebuure P. S. (1999) Local secretion of IFN-γ induces an antitumor response: comparison between T cells plus IL-2 and IFN-γ transfected tumor cells. J. Immunother. **22:** 315–323
12 Yu W. G., Yamamoto N., Takenaka H., Mu J., Tai X. G., Zou J. P. et al. (1996) Molecular mechanisms underlying IFN-γ-mediated tumor growth inhibition induced during tumor immunotherapy with rIL-12. Int. Immunol. **8:** 855–865
13 Hunter S. E., Waldburger K. E., Thibodeaux D. K., Schaub R. G., Goldman S. J. and Leonard J. P. (1997) Immunoregulation by interleukin-12 in MB49.1 tumor-bearing mice: cellular and cytokine-mediated effector mechanisms. Eur. J. Immunol. **27:** 3438–3446
14 Hirakawa M., Oike M., Masuda K. and Ito Y. (2002) Tumor cell apoptosis by irradiation-induced nitric oxide production in vascular endothelium. Cancer Res. **62:** 1450–1457
15 Manthey C. L., Perera P. Y., Salkowski C. A. and Vogel S. N. (1994) Taxol provides a second signal for murine macrophage tumoricidal activity. J. Immunol. **152:** 825–831
16 Son K. and Kim Y. M. (1995) In vivo cisplatin-exposed macrophages increase immunostimulant-induced nitric oxide synthesis for tumor cell killing. Cancer Res. **55:** 5524–5527
17 Chen Y., Yang L. and Lee T. J. (2000) Oroxylin A inhibition of lipopolysaccharide-induced iNOS and COX-2 gene expression via suppression of nuclear factor-κB activation. Biochem. Pharmacol. **59:** 1445–1457
18 Matsuda H., Kageura T., Morikawa T., Toguchida I., Harima S. and Yoshikawa M. (2000) Effects of stilbene constituents from rhubarb on nitric oxide production in lipopolysaccharide-activated macrophages. Bioorg. Med. Chem. Lett. **10:** 323–327
19 Wang C. C., Huang Y. J., Chen L. G., Lee L. T. and Yang L. L. (2002) Inducible nitric oxide synthase inhibitors of Chinese herbs. III. *Rheum palmatum*. Planta Med. **68:** 869–874
20 Goel R. K., Das Gupta G., Ram S. N. and Pandey V. B. (1991) Antiulcerogenic and anti-inflammatory effects of emodin, isolated from *Rhamnus triquerta* wall. Indian J. Exp. Biol. **29:** 230–232
21 Huang H. C., Chu S. H. and Chao P. D. (1991) Vasorelaxants from Chinese herbs, emodin and scoparone, possess immunosuppressive properties. Eur. J. Pharmacol. **198:** 211–213
22 Chang C. H., Lin C. C., Yang J. J., Namba T. and Hattori M. (1996) Anti-inflammatory effects of emodin from *Ventilago leiocarpa*. Am. J. Chin. Med. **24:** 139–142

23 Kuo Y. C., Meng H. C. and Tsai W. J. (2001) Regulation of cell proliferation, inflammatory cytokine production and calcium mobilization in primary human T lymphocytes by emodin from *Polygonum hypoleucum* Ohwi. Inflamm. Res. **50:** 73–82

24 Kuo Y. C., Tsai W. J., Meng H. C., Chen W. P., Yang L. Y. and Lin C. Y. (2001) Immune reponses in human mesangial cells regulated by emodin from *Polygonum hypoleucum* Ohwi. Life Sci. **68:** 1271–1286

25 Pechold K., Patterson N. B., Craighead N., Lee K. P., June C. H. and Harlan D. M. (1997) Inflammatory cytokines IFN-γ plus TNF-α induce regulated expression of CD80 (B7-1) but not CD86 (B7-2) on murine fibroblasts. J. Immunol. **158:** 4291–4299

26 McCarthy K. D. and De Vellis J. (1980) Preparation of separate astroglia and oligodendroglial cell cultures from rat cerebral tissue. J. Cell. Biol. **85:** 890–902

27 Pecere T., Gazzola M. V., Mucignat C., Parolin C., Vecchia F. D., Cavaggioni A. et al. (2000) Aloe-emodin is a new type of anticancer agent with selective activity against neuroectodermal tumors. Cancer Res. **60:** 2800–2804

28 Mosmann T. (1983) Rapid colorimetric assay for cellular growth and survival: application to proliferation and cytotoxicity assays. J. Immunol. Methods **65:** 55–63

29 Flick D. A. and Gifford G. E. (1984) Comparison of in vitro cell cytotoxic assays for tumor necrosis factor. J. Immunol. Methods **68:** 167–175

30 Green L. C., Wagner D. A., Glogowski J., Skipper P. L., Wishnok J. S. and Tannenbaum S. R. (1982) Analysis of nitrate, nitrite, and [15N]nitrate in biological fluids. Anal. Biochem. **126:** 131–138

31 Versteeg H. H., Nijhuis E., Van Den Brink G. R., Evertzen M., Pynaert G. N., Van Deventer S. J. et al. (2000) A new phosphospecific cell-based ELISA for p42/p44 mitogen-activated protein kinase (MAPK), p38 MAPK, protein kinase B and cAMP-response-element-binding protein. Biochem. J. **3:** 717–722

32 Trajkovic V., Markovic M., Samardzic T., Miljkovic D. J., Popadic D. and Mostarica Stojkovic M. (2001) Amphotericin B potentiates the activation of inducible nitric oxide synthase and causes nitric oxide-dependent mitochondrial dysfunction in cytokine-treated rodent astrocytes. Glia **35:**180–188

33 Miljkovic D., Markovic M., Bogdanovic N., Mostarica Stojkovic M. and Trajkovic V. (2002) Necrotic tumor cells oppositely affect nitric oxide production in tumor cell lines and macrophages. Cell. Immunol. **215:** 72–77

34 Misko T. P., Moore W. M., Kasten T. P., Nickols G. A., Corbett J. A., Tilton R. G. et al. (1993) Selective inhibition of the inducible nitric oxide synthase by aminoguanidine. Eur. J. Pharmacol. **233:** 119–125

35 Gosh S., May M. and Kopp E. B. (1998) NF-κB and REL proteins: evolutionary conserved mediators of immune responses. Annu. Rev. Immunol.**16:** 225–260

36 Chan T. C., Chang C. J., Koonchanok N. M. and Geahlen R. L. (1993) Selective inhibition of the growth of ras-transformed human bronchial epithelial cells by emodin, a protein-tyrosine kinase inhibitor. Biochem. Biophys. Res. Commun. **193:** 1152–1158

37 Zhang L., Chang C. J., Bacus S. S. and Hung M. C. (1995) Suppressed transformation and induced differentiation of HER-2/neu-overexpressing breast cancer cells by emodin. Cancer Res. **55:** 3890–3896

38 Lee H. Z. (2001) Effects and mechanisms of emodin on cell death in human lung squamous cell carcinoma. Br. J. Pharmacol. **134:** 11–20

39 Kuo P. L., Lin T. C. and Lin C. C. (2002) The antiproliferative activity of aloe-emodin is through p53-dependent and p21-dependent apoptotic pathway in human hepatoma cell lines. Life Sci. **71:** 1879–1892

40 Chen Y. C., Shen S. C., Lee W. R., Hsu F. L., Lin H. Y., Ko C. H. et al. (2002) Emodin induces apoptosis in human promyeloleukemic HL-60 cells accompanied by activation of caspase 3 cascade but independent of reactive oxygen species production. Biochem. Pharmacol. **64:** 1713–1724

41 Saura M., Zaragoza C., Bao C., McMillan A. and Lowenstein C. J. (1999) Interaction of interferon regulatory factor-1 and nuclear factor-κB during activation of inducible nitric oxide synthase transcription. J. Mol. Biol. **289:** 459–471

42 Kumar A., Dhawan S. and Aggarwal B. B. (1998) Emodin (3-methyl-1,6,8-trihydroxyanthraquinone) inhibits TNF-induced NF-κB activation, IκB degradation, and expression of cell surface adhesion proteins in human vascular endothelial cells. Oncogene **17:** 913–918

43 Jayasuriya H., Koonchanok N. M., Geahlen R. L., McLaughlin J. L. and Chang C. J. (1992) Emodin, a protein tyrosine kinase inhibitor from *Polygonum cuspidatum*. J. Nat. Prod. **55:** 696–698

44 Dell'Albani P., Santangelo R., Torrisi L., Nicoletti V. G., Vellis J. de and Giuffrida Stella A. M. (2001) JAK/STAT signaling pathway mediates cytokine-induced iNOS expression in primary astroglial cell cultures. J. Neurosci Res. **65:** 417–424

45 Samardzic T., Jankovic V., Stosic-Grujicic S. and Trajkovic V. (2001) STAT1 is required for iNOS activation, but not IL-6 production in murine fibroblasts. Cytokine **13:** 179–182

46 Chen C. W., Chang Y. H., Tsi C. J. and Lin W. W. (2003) Inhibition of IFN-γ-mediated inducible nitric oxide synthase induction by the peroxisome proliferator-activated receptor gamma agonist, 15-deoxy-delta 12,14-prostaglandin J2, involves inhibition of the upstream Janus kinase/STAT1 signaling pathway. J. Immunol. **171:** 979–988

47 Barber S. A., Fultz M. J., Salkowski C. A. and Vogel S. N. (1995) Differential expression of interferon regulatory factor 1 (IRF-1), IRF-2, and interferon consensus sequence binding protein genes in lipopolysaccharide (LPS)-responsive and LPS-hyporesponsive macrophages. Infect. Immun. **63:** 601–608

48 Konopka T. E., Barker J. E., Bamford T. L., Guida E., Anderson R. L. and Stewart A. G. (2001) Nitric oxide synthase II gene disruption: implications for tumor growth and vascular endothelial growth factor production. Cancer Res. **61:** 3182–3187

49 Cianchi F., Cortesini C., Fantappie O., Messerini L., Schiavone N., Vannacci A. et al. (2003) Inducible nitric oxide synthase expression in human colorectal cancer: correlation with tumor angiogenesis. Am. J. Pathol. **162:** 793–801

50 Feinstein D. L., Galea E., Roberts S., Berquist H., Wang H. and Reis D. J. (1994) Induction of nitric oxide synthase in rat C6 glioma cells. J. Neurochem. **62:** 315–321

51 Samardzic T., Stosic-Grujicic S., Maksimovic D., Jankovic V. and Trajkovic V. (2000) Differential regulation of nitric oxide production by increase of intracellular cAMP in murine primary fibroblasts and L929 fibrosarcoma cell line. Immunol. Lett. **71:** 149–155